A Model Predictive Control Based Generator Start-Up Optimization Strategy for Restoration with Microgrids as Black-Start Resources

Yuxuan Zhao, Zhenzhi Lin, Yi Ding, *Member, IEEE*, Yilu Liu, *Fellow, IEEE*, Lei Sun, Yong Yan

***Abstract*—Microgirds (MGs) can operate in islanded mode and serve as black-start resources for power system restoration (PSR). In this work, a model predictive control based generator start-up optimization strategy for PSR is proposed utilizing MGs as black-start resources. Firstly, the generator start-up sequence (GSUS) optimization is formulated as a mixed integer linear programming. Then the uncertainties of microgrid black-start resources (MBSRs) are modeled by discretizing the probability distribution of the forecast errors, and representative scenarios for MBSRs extracted by formulating the probability mass transportation problem. Thirdly, the generator start-up optimization strategy considering MBSRs is proposed utilizing the model predictive control (MPC) technique, in which the optimization objective is to maximize the energy capability of the power systems and minimize the load curtailment of the MGs in each looking-ahead interval. Simulations on the IEEE 118 bus system with MGs and Zhejiang provincial power system in China verify that the proposed strategy for PSR can successfully restore the power system and effectively determine the optimal GSUS.**

***Index Terms*—Black-start, microgrid, model predictive control (MPC), power system restoration (PSR), probability mass transportation problem (PMTP), scenario reduction**

NOMENCLATURE

Subscript Indexes

ω	The index of representative scenario.
ω'	The index of original scenario.
i, j, p	The indexes of non-black-start units (NBSUs), black-start units (BSUs), and buses.
i_0	The index of the targeted NBSU.
t	The index of time step.
y	The index of the MG elements.

Variables and Parameters

$P^{\max}$	Maximum, or rated, output power.
P^{crk}	Cranking power of units.
T	Overall restoration time.
$w^0/w^1/w^2/w^3$	0-1 variable representing generation stages.
$S^{\mathrm{BS}}/S^{\mathrm{NBS}}/S^{\mathrm{B}}$	Sets of BSUs/NBSUs/buses of the power system.
v^a	0-1 variable for transforming the variable inside the absolute value operator (a=1, 2, 3).
u^a/z^a	0-1 variables for restricting v^a (a=1, 2, 3).
R	Ramping rate of units.
t^{start}	Start time of units.
t^{crk}	Cranking time of units.
T^{R}	Ramping time of units.
$t^{\min}/t^{\max}$	Critical minimum/maximum time.
P^{G}	Output power of units.
$P^{\mathrm{main}}/P^{\mathrm{MG}}$	Output power of the power system/MG.
E	Stored energy of energy storage systems (ESSs).
$E^{\min}/E^{\max}$	Minimum/maximum stored energy of ESSs.
P^{f}	Predicted power.
$\delta^{\bullet}$	Forecast errors
N	Number of discretized probabilities.
N_{T}	Interval with time steps.
η/ψ	Coefficients for load curtailment.
$P^{\mathrm{UL}}/P^{\mathrm{DL}}$	Undispatchable/dispatchable loads in MG.
$P^{\mathrm{cU}}/P^{\mathrm{cD}}$	Curtailed undispatchable/dispatchable loads
$h^0/h^1/h^2/h^3$	0-1 variable restricting the load curtailment.

This work is jointly supported by National Key R&D Program of China (2016YFB0900100), National Natural Science Foundation of China (51777185), and Zhejiang Provincial Natural Science Foundation of China (LY17E070003).

Yuxuan Zhao, Zhenzhi Lin and Yi Ding are all with College of Electrical Engineering, Zhejiang University, Hangzhou 310027, China (e-mails: yuxuanzhao@aliyun.com; linzhenzhi@zju.edu.cn; yiding@zju.edu.cn).

Yilu Liu is with Department of Electrical Engineering & Computer Science, Tennessee University, Knoxville, TN, USA (e-mail: liu@utk.edu).

Lei Sun is with School of Electrical and Automation Engineering, Heifei University of Technology, Hefei 230009, China (e-mail: sunleieee@gmail.com).

Yong Yan is with Electric Power Research Institute of State Grid Zhejiang E lectric Power Company, Hangzhou 310009, China (e-mail: 55682381@qq.com).

I. INTRODUCTION

WITH the extensive applications of advanced automatic control technologies (ACTs) and information and communication technologies (ICTs) to power systems [1], the automation and intelligence level of power systems has been greatly improved, the ability to resist and cope with faults boosted, and the resilience of power systems enhanced by sophisticated and well-designed approaches [2], [3]. However, due to the increase of complexities and uncertainties, such as the integration of variable renewable energy and the demand side dynamics of loads, from the power sources, the power networks, and the demand sides, power systems are still at risk of major outages or blackouts, which should be paid more attention.

After a blackout, power system restoration (PSR) processes should be carried out to recover the system to the normal operation state. The PSR problem is a complicated process that generally involves multi-objectives, multi-stages and combinatorial nonlinear constraints [4]. So far, many research works have been conducted to optimize restoration strategies for PSR. In [5], the PSR problem is investigated based on the artificial neural networks, and several island restoration

schemes are presented for developing island restoration plans. In [6], the PSR problem is decomposed as various modules such as generation capability optimization, constraint checking, and transmission path search ones, and a mixed integer linear programming (MILP) for the generation capability optimization module is proposed to optimize the generator start-up sequence (GSUS). The linearization and simplification of overall system generation capability (GC) is firstly addressed in [6]. Since the proposed MILP is supported by multiple modules to attain the optimal GSUS, the GSUS optimization strategy in [6] can be deemed as a module based mixed integer linear programming (MBMILP). In [7], a restoration method based on "generic restoration milestones" (GRMs) is proposed, by which customized restoration plans can be generated by combining the GRMs. In [8], a black start decision-supporting system (DSS) that can automatically optimize restoration strategies and visualize the simulation results is proposed for isolated power systems. In [9], a two-stage adaptive DSS is developed to tackle online restoration problem with the constraints such as power flow, load modeling, and dynamic reserve incorporated. In [10], a framework for PSR focusing on sectionalization of the power system and GSUS is proposed, where the optimization objective aims to minimize the time when the last non-black-start unit (NBSU) is cranked.

The conventional black-start units (CBSUs) are confronted with some limitations. For example, either failures of the power plant or shortage of primary resources will result in unavailability of cranking power, which causes that the power system would not be restored. With the increasing penetration of renewable energy into power systems, research works have also been conducted considering the participation of renewable energy sources (RESs) in PSRs. In [11], a complete PSR strategy with the assist of RES is proposed and optimized by the firefly algorithm (FA) for reducing the restoration time and the unserved loads. Recently, the literature has focused on the restoration strategies with the aid of RESs in the form of microgird (MG). MG is a relatively small-scale power system that can operate in grid-connected mode and islanded mode. Integrated with various distributed generators (DGs), such as wind turbine (WT), photovoltaic (PV), dispatch unit (DU) and energy storage system (ESS), an islanded MG can provide its local loads with uninterruptable, stable and reliable power. This advantage of islanded operation can be utilized to enhance the resilience of power systems. In [12], a resilience-oriented two-stage heuristic for critical load restoration in distribution systems is proposed utilizing MGs as power sources whose uncertainties are described by a Markov chain model. In [13], considering a variety of constraints such as transient voltage and current limits of the DGs, a resiliency-based service restoration method is proposed utilizing MGs to pick up critical loads. In [14], a service restoration framework incorporating both the power support from MGs and traditional reconfiguration is proposed utilizing load data from the advanced metering infrastructure meters. It can be seen that MGs can play a significant role under emergency conditions and operations of distribution systems.

Since the recent two decades, the installed MW capacity of MG has increased significantly to the extent that cranking power requirements of NBSUs (generally ranging from several MWs to tens of MWs) can be met. Moreover, the utilization of ESS in the MG can mitigate and offset the fluctuation and randomness of RES and loads, which increases the reliability and stability of the islanded MG and its output power. In addition, the sophisticated and well-designed control strategies for MG facilitate the stable disconnection from the power system that suffered a failure and the reliable operations of islanded MGs. In summary, the capacities of MGs are sufficient enough to meet the cranking power requirements of NBSUs, and each element in the MG can be precisely dispatched by well-designed control strategies such that the securities of the islanded MGs are guaranteed. As a result, it is feasible and promising to utilize MGs to assist PSR by providing the NBSUs with sufficient and reliable cranking power. Some publications have also paid attention to using MGs as BSRs. In [15], the coordinated MGs are utilized as black-start resources (BSRs) for accelerating the disaster recovery processes of power systems. In [16], feasibility analyses on MG resiliency resources, i.e. local resource, community resource, and BSR, are performed in terms of frequency, in-rush currents, and reactive power of the system, which demonstrates that it is possible and feasible for MGs to act as BSRs on some conditions.

The CBSUs may be unavailable for PSR on some conditions such as failure of the units or lack of primary resources, while the incorporation of RESs into power system resilience enhancement and restoration has been paid much attention with the increasing proportion of RESs in power systems. Although some publications [11]-[13] have integrated RESs in the form of MGs to enhance the resilience of power systems in distribution level by picking-up critical loads or reconfiguring the distribution systems, the role of RESs in PSR in transmission level has not been fully investigated. The complete PSR strategy incorporating RESs [10] does not consider the uncertainties of RESs and the optimum cannot be guaranteed due to the heuristic optimization algorithm. Due to the increasing capabilities of MGs that aggregate RESs, ESSs and loads to enhance the resilience and reliability of power systems, the literature [14] and [15] has focused on utilization of MGs as resiliency resources so as to facilitate the PSR in transmission level. However, the restoration strategy utilizing coordinated MGs is presented for post-disaster restoration and the restoration paths of NBSUs are not optimized [14]. Moreover, the concerned MGs in [14] and [15] do not include RESs and their intrinsic uncertainties, which undermines the effectiveness of utilizing MGs as resiliency resources.

To further investigate the potential of MGs to assist PSR, a model predictive control (MPC) based generator start-up optimization strategy is proposed by utilizing the MGs as BSRs. The GSUS problem with CBSUs as the only BSRs is first addressed and formulated as a MILP model by linearizing the generation capability function. In order to utilize MGs as BSRs, uncertainties of MGs with multiple microsources (MSs) and loads are modeled as scenarios. Then the MPC technique is

applied to mitigate the inaccuracy of forecast parameters in MGs due to long forecast period, and a model predictive control based mixed integer programming (MPC-MILP) model is presented so as to incorporate MGs into GSUS optimization problem. Compared with the existing publications on PSR with participation of RESs and MGs, the proposed MPC-MILP is essentially a linear programming model, thus an optimum solution for GSUS problem can be attained. Since ignoring the fluctuation and randomness of the outputs and loads in MGs may undermine the validity of the optimized restoration strategies, the uncertainties of RESs and loads in MGs are addressed and described as scenarios. Besides, since the errors between the forecast uncertain parameters and their actual realizations of MGs will become greater as the forecast horizon increases, the MPC technique is used to mitigate the inaccuracy of forecast parameters of MGs by recursively optimizing the GSUS problem with the newly updated information of the microgrid black-start resources (MBSRs) and the concerned power system.

In summary, the major contributiona of this work can been summarized as: 1) a generator start-up optimization strategy is proposed and formulated as a MILP model for attaining the optimal GSUS; 2) an scenario generation method is proposed to model uncertainties of MGs through discretizing the probability distribution of forecast errors (PDFEs); 3) based on the probability mass transportation problem (PMTP), a linear programming scenario reduction (LPSR) method is proposed to efficiently deal with a large number of original uncertainty scenarios with unequal probabilities, 4) the MPC technique is first applied to PSR to mitigate the inaccuracy of the forecast power of MGs caused by long forecast time horizon (FTH) and a MPC-MILP model for integrating MBSRs into the GSUS optimization problem is proposed.

The rest of this work is structured as follows. In Section II, a novel MILP model for addressing the GSUS problem is proposed. The feasibility of MBSRs is analyzed and the scenario based uncertainty management algorithms are presented in Section III. Section IV introduces the MPC technique and presents the MPC based GSUS optimization strategy. Simulations are performed in Section V. Discussions and comparisons on the proposed methods are made in Section VI. Finally, conclusions of this work are highlighted in Section VII.

II. A MILP Model for GSUS Optimization

At the early stage of restoration, cranking power should be provided to NBSUs that are generally thermal power plants as soon as possible by black-start units (BSUs) [4]. However, NBSUs cannot be restored simultaneously at that stage due to restrictions such as the limited megawatt (MW) capacity of BSUs and the critical minimum/maximum times of NBSUs. Therefore, it is of significance to determine the optimal GSUS for maximizing restoration benefits. Generally, the objective of the GSUS problem is to maximize the overall energy capability in MWh (i.e., the difference between the total system restored energy and the required start-up energy of NBSUs) over the system restoration time T. In [6], this objective is linearized and simplified as

$$\min \sum_{i\in S^{\mathrm{NBS}}} (P_i^{\max} - P_i^{\mathrm{crk}}) t_i^{\mathrm{start}} \tag{2}$$

where S^{NBS} represents the set of NBSUs; $P\max\ i$ and $P\mathrm{crk}\ i$ represent the rated output power and cranking power requirement of NBSU i, respectively; $t\mathrm{start}\ i$ represents the start time of NBSU i, i.e., the time when NBSU i gets cranking power.

In order to optimize GSUS, the MW capacity of NBSUs and BSUs should be first modeled. The MW capacity of a unit can be separated into four stages, as shown in Fig. 1. In Fig. 1, the black solid line above/below t axis represents the total output power/cranking power of the unit, whereas the red solid line is the actual output power of the unit synthesized by the total output power and cranking power. Then the MW capacity of a unit can be expressed by introducing four variables (i.e., $w^0/w^1/w^2/w^3$) in each time t, as shown in Fig. 1. Each variable corresponds to one stage: if the variable is equal to 1, it means that the output power of the unit is in the very stage; otherwise, not in this stage. For these variables, the following constraints should be respected.

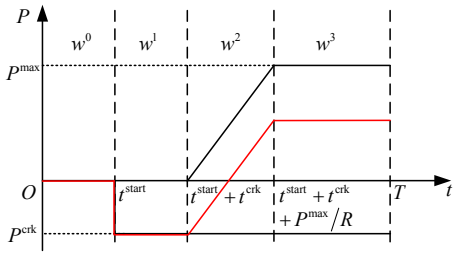

Fig. 1. Generation capability function of units

$$w_{it}^0 + w_{it}^1 + w_{it}^2 + w_{it}^3 = 1 \quad (\forall i \in S^{\mathrm{BS}} \bigcup S^{\mathrm{NBS}};\ t = 0,...,T) \tag{3}$$

$$w_{it}^0 \le w_{i(t+1)}^0 + w_{i(t+1)}^1 \quad (\forall i \in S^{\mathrm{BS}} \bigcup S^{\mathrm{NBS}};\ t = 0,...,T-1) \tag{4}$$

$$w_{it}^1 \le w_{i(t+1)}^1 + w_{i(t+1)}^2 \quad (\forall i \in S^{\mathrm{BS}} \bigcup S^{\mathrm{NBS}};\ t = 0,...,T-1) \tag{5}$$

$$w_{it}^2 \le w_{i(t+1)}^2 + w_{i(t+1)}^3 \quad (\forall i \in S^{\mathrm{BS}} \bigcup S^{\mathrm{NBS}};\ t = 0,...,T-1) \tag{6}$$

$$w_{it}^3 \le w_{i(t+1)}^3 \quad (\forall i \in S^{\mathrm{BS}} \bigcup S^{\mathrm{NBS}};\ t = 0,...,T-1) \tag{7}$$

$$w_{i0}^0 = 1 \quad (\forall i \in S^{\mathrm{NBS}}) \tag{8}$$

$$w_{it}^0 = 0 \quad (\forall i \in S^{\mathrm{BS}};\ t = 0,...,T-1) \tag{9}$$

$$w_{iT}^3 = 1 \quad (\forall i \in S^{\mathrm{BS}} \bigcup S^{\mathrm{NBS}}) \tag{10}$$

$$\sum_{t=0}^{T-1} \left| w_{it}^1 - w_{i(t+1)}^1 \right| = 2 \quad (\forall i \in S^{\mathrm{NBS}}) \tag{11}$$

$$\sum_{t=0}^{T-1} \left| w_{it}^1 - w_{i(t+1)}^1 \right| = 1 \quad (\forall i \in S^{\mathrm{BS}}) \tag{12}$$

$$\sum_{t=0}^{T-1} \left| w_{it}^2 - w_{i(t+1)}^2 \right| = 2 \quad (\forall i \in S^{\mathrm{BS}} \bigcup S^{\mathrm{NBS}}) \tag{13}$$

$$\sum_{t=0}^{T} w_{it}^0 = t_i^{\mathrm{start}} - 1 \quad (\forall i \in S^{\mathrm{BS}} \bigcup S^{\mathrm{NBS}}) \tag{14}$$

$$\sum_{t=0}^{T} w_{it}^1 = t_i^{\mathrm{crk}} \quad (\forall i \in S^{\mathrm{BS}} \bigcup S^{\mathrm{NBS}}) \tag{15}$$

$$\sum_{t=0}^{T} w_{it}^2 = T_i^{\mathrm{R}} \quad (\forall i \in S^{\mathrm{BS}} \bigcup S^{\mathrm{NBS}}) \tag{16}$$

Equation (3) represents that each unit could be in only one stage at each time t. Equations (4) to (7) restrict the values of the variables (i.e., w^0/w^1/w^2/w^3) at each stage of units; they guarantee that once one unit reaches a specific stage, it will not go back and will stay in the corresponding state until it reaches the next stage. Equation (7) indicates that all the NBSUs are out of service and the cranking power is unavailable at the beginning of the restoration. Equation (9) indicates that the BSU can be restarted by itself, i.e., the BSU will not undergo the first stage corresponding to w^0. Equation (10) indicates that all the units are restored at the end of the restoration. Equations (11) to (13) restrict the times of state changes of different units. The state of each unit can only change once or twice. For example, if $w_{i\mathrm{g}}^1$ ($w_{i\mathrm{g}}^2$) of the NBSU changes from 0 to 1, it cannot change from 1 to 0 until $w_{i\mathrm{g}}^2$=1 ($w_{i\mathrm{g}}^3$=1); once $w_{i\mathrm{g}}^2$=1 ($w_{i\mathrm{g}}^3$=1), $w_{i\mathrm{g}}^1$ ($w_{i\mathrm{g}}^2$) changes from 1 to 0. In other words, the state of $w_{i\mathrm{g}}^1$ ($w_{i\mathrm{g}}^2$) of the NBSU changes twice. Similar analyses can be made for $w_{i\mathrm{g}}^2$ of the BSU, and the constraint for $w_{i\mathrm{g}}^2$ of the BSU is included in (12). According to (3)-(7) and (9), w_{i0}^1 of the BSU equals 1. Thus $w_{i\mathrm{g}}^1$of the BSU can only changes once, i.e. from 1 to 0, as constrained by (12). Equations (14) to (16) restrict the duration time of each stage, i.e., the duration times of stages shown in (14), (15), and (16) are restricted by the start time, cranking time and ramping time, respectively. Absolute value operators (AVOs) in (11) to (13) make the problem intractable, so binary variables *va it* are introduced to represent the variables inside AVOs (a=1, 2, 3 for (11), (12), (13) respectively). For example, $|w1\ it–w1\ i(t+1)|$ can be represented as $v1\ it$ that respects the following constraints.

$$\begin{cases} 0 \le v_{it}^1 - (w_{it}^1 - w_{i(t+1)}^1) \le 2z_{it}^1 \\ 0 \le v_{it}^1 - (w_{i(t+1)}^1 - w_{it}^1) \le 2u_{it}^1 \quad (t = 0,...,T-1) \\ u_{it}^1 + z_{it}^1 = 1 \end{cases} \tag{17}$$

Then the output power of a unit can be expressed as:

$$P_{it}^{\mathrm{G}} = -(w_{it}^1 + w_{it}^2 + w_{it}^3)P_i^{\mathrm{crk}} + w_{it}^2 R_i (t - t_i^{\mathrm{start}} + 1 - t_i^{\mathrm{crk}}) + w_{it}^3 P_i^{\max} \quad (\forall i \in S^{\mathrm{BS}} \bigcup S^{\mathrm{NBS}};\ t = 0,...,T). \tag{18}$$

The quadratic term in (18) can also be linearized by introducing extra binary variables y_{it}, then equation (18) can be expressed as:

$$P_{it}^{\mathrm{G}} = -(w_{it}^1 + w_{it}^2 + w_{it}^3)P_i^{\mathrm{crk}} + w_{it}^2 R_i (t - t_i^{\mathrm{crk}}) - R_i \sum_{t=0}^{T} y_{it} + w_{it}^3 P_i^{\max} \quad (\forall i \in S^{\mathrm{BS}} \bigcup S^{\mathrm{NBS}};\ t = 0,...,T), \tag{19}$$

where $y_{it} = w_{it}^2 w_{it}^0$ should respect the following constraint.

$$\begin{cases} y_{it} \ge w_{it}^2 + w_{it}^0 - 1 \\ y_{it} \le w_{it}^0 \\ y_{it} \le w_{it}^2 \end{cases} \quad (\forall i \in S^{\mathrm{BS}} \bigcup S^{\mathrm{NBS}};\ t = 0,...,T) \tag{20}$$

The overall output power of the system at each time step t should be non-negative, as

$$P_t^{\mathrm{main}} = \sum_{i \in S^{\mathrm{NBS}} \bigcup S^{\mathrm{BS}}} P_{it}^{\mathrm{G}} \ge 0 \quad (t = 0,...,T). \tag{21}$$

For the NBSUs, the critical minimum and maximum time constraints should be met, as

$$t_i^{\min} \le t_i^{\mathrm{start}} \quad (\forall i \in S^{\mathrm{NBS}}) \tag{22}$$

$$t_i^{\mathrm{start}} \le t_i^{\max} \quad (\forall i \in S^{\mathrm{NBS}}). \tag{23}$$

Besides, the generator start-up time should be at least larger than the energizing time $\tau_{\sigma(p,i)^{m^*}}$ of the transmission path from BSU p to NBSU i, as

$$\tau_{\sigma(p,i)^{m^*}} \le t_i^{\mathrm{start}} \quad (\forall i \in S^{\mathrm{NBS}}). \tag{24}$$

The energizing time $\tau_{\sigma(p,i)^{m^*}}$ of the restoration path can be attained from the presented path optimization model on the basic of the node degree of complex network theory.

Restoring NBSUs entails an appropriate restoration path. The determination of an optimal restoration path for restoring NBSU is to find a set of transmission lines connecting buses that can minimize the risks of overvoltage resulting from energizing unloaded lines and the line energization times. On the other hand, the optimization of GSUS problem should not only identify an optimal start-up sequence that can maximize the restoration benefit, but also facilitate the subsequent restoration processes so as to reduce the restoration time of the entire power system and the overall unserved energy. In other words, appropriate restoration paths of NBSUs should decrease the overvoltage of energizing lines, reduce the energization time, and facilitate the subsequent restoration. In order to taking into account these considerations, the restoration path optimization model is proposed. In complex network theory, the degree of a node denotes the number of the neighbor nodes of that node [17]. The node degree reflects the connectivity level of a specific node to other parts of the graph. The larger the degree of a node is, the more important that node is. However, when the degrees of two nodes are equal to each other, it is difficult to identify which node is more important. Therefore, the node degree is improved by considering the degree contributions of neighbor nodes and then utilized to evaluate the bus importance of power system in this work. The improved bus (node) degree of power system is defined as:

$$d_i^{\mathrm{imp}} = d_i^{\mathrm{self}} + \sum_{j \in S_i^{\mathrm{nb}}} d_j^{\mathrm{self}} C_{ji} \tag{25}$$

where $d$imp i and $d$self i denotes the improved bus degree and bus degree of bus i, respectively [18]; Snb i denotes the set of neighbor buses of bus i; the second term of the right side can be regarded as degree contributions of the neighbor buses; C_{ji} is a coefficient denoting the contribution level of neighbor node j to node i. The larger the charging capacitance of a line is, the more serious the overvoltage phenomenon is. Thus, the capacitances of lines are considered in (25), i.e., $C_{ij} = 1/[c_{ji} \sum_{p \in S_j^{\mathrm{nb}}} (1/c_{pj})]$ where c_{ij} represents the capacitance of line (i, j). Since c_{ji}=c_{ij}, the improved node degree can be expressed as:

$$d_i^{\mathrm{imp}} = d_i^{\mathrm{self}} + \sum_{j \in S_i^{\mathrm{nb}}} \frac{d_j^{\mathrm{self}}}{c_{ij} \sum_{p \in S_j^{\mathrm{nb}}} (1/c_{pj})}, \quad (\forall i \in S^{\mathrm{B}}) \tag{26}$$

where S^{B} represents the set of buses of the power system.

The injection power of a bus reflects the capacity of that bus

to transfer electric power to other buses. Incorporating the improved bus degree and the ratio of the maximum injection active power of bus i Pin i to the base power P^{B} (named as power transfer factor in this work), the importance of a bus can be evaluated by:

$$D_i = d_i^{\mathrm{imp}} \Big/ \max_{j \in S^{\mathrm{B}}} d_j^{\mathrm{imp}} + \lambda\, \varepsilon_i \Big/ \max_{j \in S^{\mathrm{B}}} \varepsilon_j \quad (\forall i \in S^{\mathrm{B}}) \tag{27}$$

where $\varepsilon_i = P_i^{\mathrm{in}} \big/ P^{\mathrm{B}}$ represents the power transfer factor of bus i; D_i represents the importance of bus i; λ is a coefficient. As shown in (27) the bus degree and line capacitance are integrated into the bus importance index. The bus degree indicates the connectivity level of a bus to its neighbor buses, the line capacitance is related to the overvoltage caused by energizing an unloaded line, and the power transfer factor reflects the capacity of a bus to transfer electric power to other buses. Thus incorporating the proposed bus importance into restoration path optimization can facilitate the subsequent restoration and mitigate the overvoltage. With the bus importance and the energization time considered, the path optimization model can be formulated as (28).

$$\min_{\sigma(p,i)^m} r_{\sigma(p,i)^m} = 1 \big/ \tau_{\sigma(p,i)^m} + \gamma \sum_{j \in \sigma(p,i)^m, j \neq i,p} 1 \big/ D_j \tag{28}$$

where $\sigma(p,i)^m$ represents the m^{th} restoration path from BSU p to NBSU i; $\tau_{\sigma(p,i)^m}$ represents the energization time of the m^{th} restoration path from BSU p to NBSU i; γ is a coefficient. As seen from (28), the value of the first term will decrease and the value of the second one will likely increase as the line number (or bus number) of a path rises. As a result, the optimal restoration path that takes into account the energization time and bus importance can be attained by minimizing (28).

The bus importance, as well as the overall bus importance and energization time of one path in (28) can be easily calculated. $\sigma(p,i)^m$ is the decision variable and the solution domain of (28) is a finite and countable set, thus it is tractable to attain the minimum of the objective. The index of the solution of (28) is denoted as:

$$m^* = \arg \min_{\sigma(p,i)^m} r_{\sigma(p,i)^m} \tag{29}$$

According to the path optimization model (28), optimal restoration paths $\sigma(p,i)^{m^*}$ can be determined and then the energization time $\tau_{\sigma(p,i)^{m^*}}$ of that path is imposed upon (24).

Constraints to voltage and reactive power are checked before energizing a certain transmission line or cranking a NBSU. If the constraints are not respected, it means that the BSRs provided by BSUs and NBSUs already restored are insufficient at the current time step. Therefore, an extra time constraint can be added into the model and it will be re-solved.

The model in (2)-(24) for the GSUS problem can be linearized as a MILP, and then utilized to optimize the GSUS. Recently, utilization of MGs to aid PSR has been paid much attention [15], [16]. In the following sections, the feasibility of MBSRs is analyzed, and then a PDFE and PMTP based approach proposed to model the uncertainties of MBSRs. Finally, an improved MILP based on MPC is proposed so as to incorporate MGs into GSUS optimization problem.

III. MBSR Modeling Based on PDFE and PMTP

A. Feasibility of Microgrid Black-Start Resources

Although the capacity of a single MG has been increasing rapidly such that it can met the cranking power requirements of NBSUs, small-scale MGs that are geographically adjacent can also be aggregated as multi-microgrid (MMG) or microgrid cluster (MGC) that also has a large MW capacity so as to provide NBSUs with sufficient cranking power [19]. However, the GSUS problem of the PSR is mainly focused on in this work and both the MMG and MGC are regarded as a single MG despite their differences. On the other hand, the reactive power can be provided by not only DUs in the MG but also the inverters of MSs of the MG [15], [16], and [20]. Moreover, the fluctuation and randomness can be mitigated and offset by the ESS in MG to the extent that the reliability and stability of the islanded MG are maintained. Therefore, in terms of the MW capacity, it is feasible for the MGs to act as BSRs and provide enough cranking power to NBSUs after a blackout.

A MG typically consists of four types of MSs, i.e., WT, PV, DU, and ESS. The RES (WT and PV) MSs and ESS MS are interfaced with MG by inverters. MSs of a MG are controlled and managed by the microgird central controller (MGCC) [21]. In general, the converter controllers of MSs have three control mode: PQ (active power and reactive power) control, Vf (voltage and frequency) control, and droop control [22]. When a failure of a power system is detected, MGs are disconnected from the concerned power system (maingrid) under the control of MGCCs and operate in islanded mode. The cranking power of NBSUs can be deemed as local loads of an islanded MG. The islanded MG is coordinated by adjusting the output power of MSs and loads through MGCC to ensure that the restoration requirements, such as cranking power of NBSUs, voltage and frequency stability of the coalition of the maingrid and MGs, are satisfied. Since at least one master inverter with stable output power is required for the islanded MG to set voltage and frequency references, the RES inverter should operate in PQ control mode and the ESS inverter or DU should operate in Vf control mode before the maingrid could operate stably [21]. After the maingrid could provide the voltage and frequency reference, the Vf controlled inverters could be transferred into PQ control. The fluctuation and randomness of MSs and loads during restoration period can be coordinated and controlled by the MGCC through the droop characteristics of inverters. The above control strategies guarantee that the MGs can provide the NBSUs with cranking power and operate stably during restoration.

In summary, it is feasible, in terms of capacities and control strategies, for MGs to act as BSRs so as to provide cranking power to NBSUs.

B. Scenario Generation Based on Discretization of PDFE

Before a MG is utilized as a BSR, the output power of its RESs should be forecast over a time period T_{p}. Only if the forecast net power of an islanded MG in a period of time T_{f} (that is at least longer than the cranking time of the targeted

NBSU) is large enough, the MG can be utilized as the BSR. However, the actual output power of weather-dependent MSs in MG is of randomness and intermittency and is usually not the same as the predicted values. Moreover, the power supply to local loads in the MG might be considered when the restoration plan is made and carried out. In order to model the power of WT, PV and loads of MGs, a scenario generation method is proposed by discretizing PDFE and then representative scenarios are selected by formulating and optimizing the PMTP.

Considering fluctuations of wind, solar and loads, the actual output power can be denoted as the sum of the predicted ones and forecast errors (FEs), as

$$P_{yt\omega'} = P_{yt}^{\mathrm{f}} + \delta_{yt\omega'} \quad (y=1,2,3;\ t=t_{\mathrm{f}},...,t_{\mathrm{f}}+T_{\mathrm{f}}) \tag{30}$$

where y=1, 2, and 3 represent WT, PV and loads respectively.

Normal distribution can be utilized to describe the FEs [23]-[25]. The PDFE of each uncertain variable is discretized into intervals and the probability of each interval is equal to the cumulative probability in this interval [26], which can be expressed as:

$$\mathbf{V}_{yt} = \{(\delta_{yt}^{1},\rho_{y}^{1}),...,(\delta_{yt}^{N_y},\rho_{y}^{N_y})\},(y=1,2,3;\ t=t_{\mathrm{f}},...,t_{\mathrm{f}}+T_{\mathrm{f}}) \tag{31}$$

$$\mathbf{p}_{y}^{\mathrm{err}} = [\rho_{y}^{1},...,\rho_{y}^{N_y}]^{\mathrm{T}} \quad (y=1,2,3) \tag{32}$$

where $\mathbf{V}_{yt}$ represents the set of pairs of the FE and probability $(\delta_{yt}^{\bullet},\rho_{y}^{\bullet})$; $\mathbf{p}_{y}^{\mathrm{err}}$ represents a probability vector and the sum of its elements is equal to 1.

Based on the probability discretization from (31) to (32), the error scenario space containing the errors of variables associated with wind power, solar power and loads can be generated by the Monte Carlo method and expressed as:

$$S_{\mathrm{e}}(t_{\mathrm{f}}) = \prod_{t=t_{\mathrm{f}}}^{t_{\mathrm{f}}+T_{\mathrm{f}}} (\mathbf{V}_{1t} \times \mathbf{V}_{2t} \times \mathbf{V}_{3t}) \tag{33}$$

where $S_{\mathrm{e}}(t_{\mathrm{f}})$ represents the error scenario space from t_{f} to t_{f}+T_{f} with the dimension of $T_{\mathrm{f}}\times 3$.

After the error scenarios are attained, the uncertainty scenario space $S_0(t_{\mathrm{f}})$ containing the output power of RESs and load power of the MG can be attained according to (30). The probability of each uncertainty scenario can be represented by

$$p_{\omega'}^{\mathrm{orig}} = \prod_{t=t_{\mathrm{f}}}^{t_{\mathrm{f}}+T_{\mathrm{f}}} \prod_{y=1}^{3} (\boldsymbol{\alpha}_{yt\omega'}^{\mathrm{T}} \mathbf{p}_{y}^{\mathrm{err}}) \Big/ \sum_{\omega'\in S_0(t_{\mathrm{f}})} \prod_{t=t_{\mathrm{f}}}^{t_{\mathrm{f}}+T_{\mathrm{f}}} \prod_{y=1}^{3} (\boldsymbol{\alpha}_{yt\omega'}^{\mathrm{T}} \mathbf{p}_{y}^{\mathrm{err}}) \tag{34}$$

where $\boldsymbol{\alpha}_{yt\omega'}^{\mathrm{T}}$ represents the unit vector for scenario selection, in which only the entry corresponding to the position of the very scenario ω' is 1, and other entries are 0.

C. Representative Scenario Selection by PMTP

It can be seen from (33) that the number of scenarios increases exponentially. Too many scenarios make intractable the problem of modeling and optimization of GSUS with MBSRs. In order to improve the computational efficiency, representative scenarios that can capture the main characteristics of the majority of scenarios should be selected. Various scenario reduction methods have been proposed, such as the *k*-means cluster method, the SCENRED2 tool in GAMS (The General Algebraic Modeling System) [27] and the fast forward selection [28]. However, these methods have their limitations. For example, the *k*-means method cannot tackle scenarios with unequal probability, and the SCENRED2 tool and fast forward selection are less efficient when the original superset of scenarios is large [29], [30]. The PMTP based LPSR method can efficiently deal with the unequal probability and a large number of original scenarios, and has been applied to fields such as Voronoi diagram and chance constrained portfolio optimization [30]. Generally, the original uncertainty scenarios of MBSRs are characterized as large quantities and unequal probabilities, therefore the PMTP based LPSR is firstly proposed in power systems to extract a small number of representative scenarios of MBSRs.

The PMTP based LPSR consists of three main steps. The first step initializes a subset of representative scenarios by any methods such as random selection or *k*-means method. The number of representative scenario is a user-defined value and should be pre-specified before this step. Then a subset of the desired number of representative scenarios can be attained. The representative scenarios can be viewed as cluster center that represents a certain number of original scenarios (named as scenario cluster) according to their distance to the cluster centers. The second step optimizes the transportation plan by solving PMTP that minimizes probabilistic distance between the original superset of scenarios and the reduced subset of representative scenarios. The third step reevaluates the probabilistic distance until it converges by altering the cluster centers within their scenario clusters. The PMTP based LPSR can be illustrated by Fig. 2 utilizing random selection and *k*-means method respectively, wherein the desired number of representative scenarios is set as three.

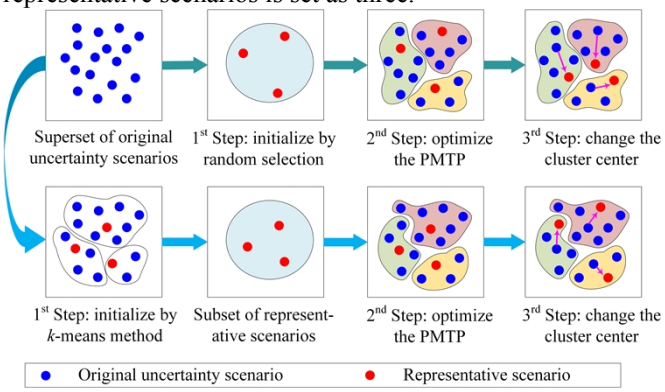

Fig. 2. Illustration of the PMTP based LPSR utilizing random selection and k-means method respectively

The PMTP that selects representative uncertainty scenarios for MBSRs can be formulated as:

$$\min \sum_{\omega\in S(t_{\mathrm{f}})} \sum_{\omega'\in S_0(t_{\mathrm{f}})} c_{\omega\omega'}\pi_{\omega\omega'} \tag{35}$$

$$s.t.: \sum_{\omega\in S(t_{\mathrm{f}})} \pi_{\omega\omega'} = p_{\omega'}^{\mathrm{orig}} \tag{36}$$

$$\sum_{\omega'\in S_0(t_{\mathrm{f}})} \pi_{\omega\omega'} = p_{\omega}^{\mathrm{rep}} \tag{37}$$

$$\pi_{\omega\omega^{i}} \geq 0, \forall\omega\in S(t_{\mathrm{f}}) \quad \forall\omega'\in S_0(t_{\mathrm{f}}) \tag{38}$$

where $S(t_f)$ represents the representative scenarios space; $c_{\omega\omega'}$ represents the transportation cost of moving $\omega' \in S_0(t_f)$ to $\omega \in S(t_f)$, and is generally called as transportation distance or cost function; $p_{\omega'}^{orig}$ and p_{ω}^{rep} represent the probabilities of the original and representative scenarios, respectively; $\pi_{\omega\omega'}$ is the decision variables representing the transportation plan, and is the joint probability distribution on $S(t_f) \times S_0(t_f)$ [31]. In this work, $c_{\omega\omega'} = \sum_{y=1}^{3} \left\| P_{yt\omega} - P_{yt\omega'} \right\|_2$.

The processes of the PDFE and PMTP based uncertainty modeling for MBSR can be shown in Fig. 3. The processes of the uncertainty modeling for MBSR can be summarized as follows.

1) generate the error scenario space by discretizing the PDFE of uncertainty parameters and the uncertainty scenario space, and calculate the probability of uncertainty scenarios;

2) initialize a subset of representative scenarios by *k*-means method from the original superset of uncertainty scenarios;

3) optimize the PMTP, and then the scenario clusters can be attained from the transportation plan and the probability p_{ω}^{rep} of representative scenario from the marginal distribution of $\pi_{\omega\omega^i}$ on $S(t_f)$;

4) alter the representative scenario (cluster center) of each scenario cluster and identify the one leading to the minimum transportation cost within this cluster;

5) update the subset of the identified representative scenarios and re-calculate the probabilistic distance (the objective of PMTP) utilizing the known transportation plan;

6) if the probabilistic distance converges, the representative scenarios of MBSRs can be attained; otherwise, repeat steps 3) to 5) until the objective value of PMTP converges.

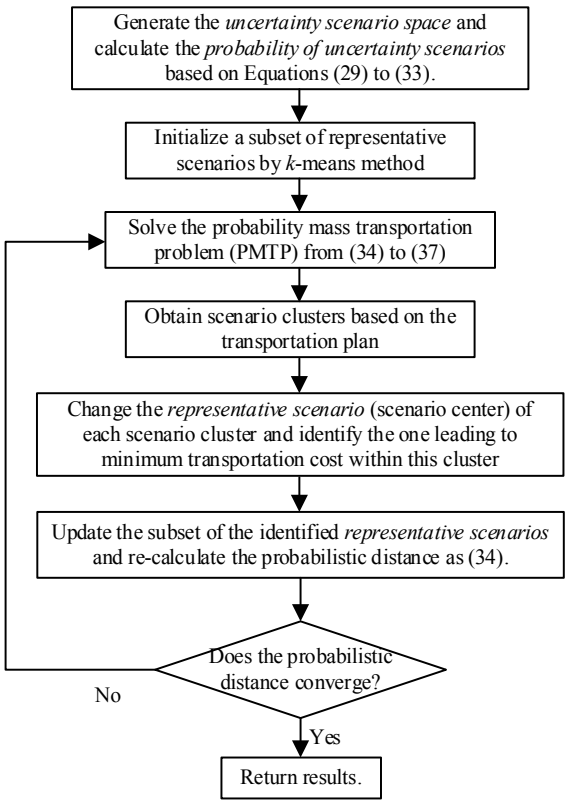

Fig. 3. The flow chart of the proposed PMTP based LPSR

IV. MPC Based GSUS Optimization with MBSRs

A. Model Predictive Control

When restoring the power system, the FEs of wind power, solar power and loads of the MBSRs will become larger with the increase of FTH. At the end of the FTH, the actual black-start power that the MG can provide may not be the same as those values at the time step when the restoration model is optimized, and the GSUS problem optimized once only in the initial time might not be the globally optimal one. In order to deal with the inaccuracy of forecast power caused by long FTH, the MPC technique is introduced into the restoration strategy.

The control technique, in which a problem is optimized recursively in a finite-moving-horizon of intervals by forecast parameters and then only the attained control scheme in the first interval is applied to the problem, is called as MPC or receding horizon control (RHC) [32]. Recently, the MPC technique has been applied to formulate economic dispatch and energy management frameworks of MG [33], [34], and voltage regulation strategy of ESSs [35]. The MPC technique can consider the latest forecast parameters by recursively optimizing the relevant problem with the newly updated data, thus it can reduce the impacts of uncertainties of MBSRs and achieve a globally optimal restoration scheme. Applying the MPC technique, the uncertainty parameters in the MG and the state of NBSUs in the power system are updated in each time interval, and then the GSUS problem can be recursively optimized in each interval. Since the overall restoration time of the system is finite, and the number of unrestored NBSUs optimized in each interval in the look-ahead planning horizon is decreasing with the successive restoration scheme, the shrinking horizon control (SHC), a variant of the MPC technique [36], is utilized in this work to optimize the generator start-up strategy with MBSRs. In the SHC technique, the look-ahead planning horizon reduces with successive restoration schemes, which is more efficient for the GSUS problem than the original MPC with fixed planning horizon.

The proposed SHC technique for GSUS problem can be illustrated by Fig. 4. As shown in Fig. 4, the uncertainties of WT, PV and loads of MBSRs are managed T_f–N_T ahead the k^{th} planning horizon T–(k–1)N_T. Due to the exponential increase of scenario number, the uncertainty scenarios are generated and representative scenarios selected T_f–N_T ahead the k^{th} planning horizon T–(k–1)N_T in a relative shorter interval T_f (that should be no less than N_T), and then each representative scenario is extended with the forecast values of the subsequent planning horizon T–kN_T. After the scenario extension processes, the GSUS optimization model is solved for the k^{th} interval N_T considering a look-ahead planning horizon T–kN_T, and a sequence of unit start-up and load curtailment schemes is

attained but only the attained schemes in the k^{th} interval will be carried out. Both uncertainty management and optimization solving processes are performed in advance within the period T_{f}–N_{T} so as to reserve enough time to implement the restoration actions. The scenario extension processes and the SHC (MPC) based GSUS optimization are repeated for GSUS optimization until all NBSUs are restored.

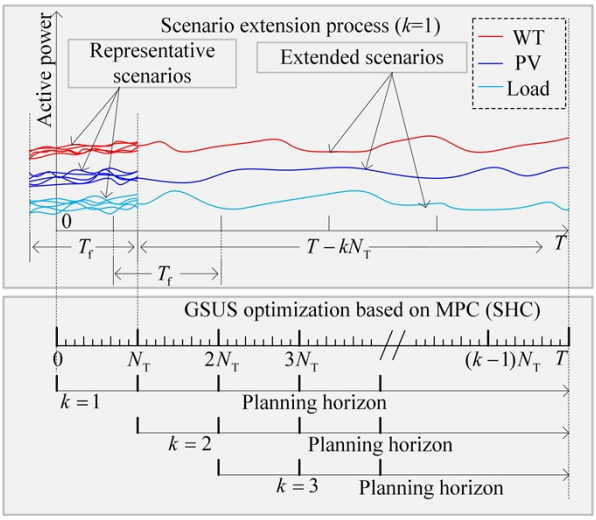

Fig. 4. Schematic diagram of the MPC technique for GSUS optimization

B. MPC Based GSUS Optimization with MBSRs

The power system aims to maximize its energy capability, but for the MBSRs the welfare of their local customer should be considered. Although the local loads should be sustained by the MGs, it might be inevitable for the MG to selectively curtail local loads for PSR after a big blackout. Generally, the local customer consists of dispatchable loads (DLs) and undispatchable loads (ULs) that are with perfect forecast values. The energy losses of the curtailed loads over the restoration period should be minimized, as:

$$\min \sum_{t=0}^{T} \sum_{\omega \in S(t_{\text{f}})} p_{\omega}^{\text{rep}} \left(P_{t\omega}^{\text{cD}} + \psi P_{t\omega}^{\text{cU}} \right). \tag{39}$$

The curtailment of DLs and ULs can be expressed as (40) and (41) respectively.

$$P_{t\omega}^{\text{cD}} = \begin{cases} P^{\text{UL}} + P_{t\omega}^{\text{DL}} - P_{t\omega}^{\text{main}} - P_{t\omega}^{\text{MG}} \\ \quad if \quad 0 < P_{t\omega}^{\text{main}} + P_{t\omega}^{\text{MG}} - P^{\text{UL}} < P_{t\omega}^{\text{DL}} \\ P_{t\omega}^{\text{DL}} \quad if \quad P_{t\omega}^{\text{main}} + P_{t\omega}^{\text{MG}} - P^{\text{UL}} \le 0 \\ 0 \quad other \\ \qquad (\forall \omega \in S(t_{\text{f}});\ t = 0,...T) \end{cases} \tag{40}$$

$$P_{t\omega}^{\text{cU}} = \begin{cases} P^{\text{UL}} - P_{t\omega}^{\text{main}} - P_{t\omega}^{\text{MG}} \quad if \quad P_{t\omega}^{\text{main}} + P_{t\omega}^{\text{MG}} - P^{\text{UL}} \le 0 \\ 0 \quad other \\ \qquad (\forall \omega \in S(t_{\text{f}});\ t = 0,...T) \end{cases} \tag{41}$$

Equations (40) and (41) can be further modeled as mixed integer formulation by introducing binary variables h_{tw}^{g}, as:

$$P_{t\omega}^{\text{cD}} = Mh_{t\omega}^{0} + P_{t\omega}^{\text{DL}} h_{t\omega}^{1} + (P_{t\omega}^{\text{DL}} + P^{\text{UL}} - P_{t\omega}^{\text{main}} - P_{t\omega}^{\text{MG}}) h_{t\omega}^{2} \quad (\forall \omega \in S(t_{\text{f}});\ t = 0,...T) \tag{42}$$

$$P_{t\omega}^{\text{cU}} = (P^{\text{UL}} - P_{t\omega}^{\text{main}} - P_{t\omega}^{\text{MG}}) h_{t\omega}^{1} \quad (\forall \omega \in S(t_{\text{f}});\ t = 0,...T) \tag{43}$$

$$h_{t\omega}^{0} + h_{t\omega}^{1} + h_{t\omega}^{2} + h_{t\omega}^{3} = 1 \quad (\forall \omega \in S(t_{\text{f}});\ t = 0,...T) \tag{44}$$

$$(P_{t\omega}^{\text{main}} + P_{t\omega}^{\text{MG}}) h_{t\omega}^{0} \le 0 \quad (\forall \omega \in S(t_{\text{f}});\ t = 0,...T) \tag{45}$$

$$0 \le (P_{t\omega}^{\text{main}} + P_{t\omega}^{\text{MG}}) h_{t\omega}^{1} \le P^{\text{UL}} \quad (\forall \omega \in S(t_{\text{f}});\ t = 0,...T) \tag{46}$$

$$P^{\text{UL}} h_{t\omega}^{2} \le (P_{t\omega}^{\text{main}} + P_{t\omega}^{\text{MG}}) h_{t\omega}^{2} \le (P^{\text{UL}} + P_{t\omega}^{\text{DL}}) h_{t\omega}^{2} \quad (\forall \omega \in S(t_{\text{f}});\ t = 0,...T) \tag{47}$$

$$(P^{\text{UL}} + P_{t\omega}^{\text{DL}}) h_{t\omega}^{3} \le (P_{t\omega}^{\text{main}} + P_{t\omega}^{\text{MG}}) h_{t\omega}^{3} \quad (\forall \omega \in S(t_{\text{f}});\ t = 0,...T) \tag{48}$$

where M is a big enough positive number and $Mh_{t\omega}^{0}$ in (42) is a penalty for guaranteeing that the constraint to the restoration power is respected. Equations (42) to (48) restrict the loads curtailment in their corresponding ranges. Constraints to the WTs, PVs, DUs and ESSs of MBSRs should also be met [37].

Finally, taking into account the energy losses of loads of MBSRs, the GSUS optimization model in the k^{th} interval can be expressed as a MPC-MILP:

$$\min \sum_{i \in S^{\text{NBS}} \setminus \bigcup_{l=0}^{k-1} S_l^{\text{start}}} (P_i^{\max} - P_i^{\text{crk}}) t_i^{\text{start}} + \eta \sum_{t \in S_{\text{T}}(k)} \sum_{\omega \in S(t_{\text{f}})} p_{\omega} \left(P_{t\omega}^{\text{cD}} + \psi P_{t\omega}^{\text{cU}} \right) \tag{49}$$

Subject to:

$$t_{\text{f}} = (k-1)N_{\text{T}} \tag{50}$$

$$w_{it}^{0} + w_{it}^{1} + w_{it}^{2} + w_{it}^{3} = 1 \quad (\forall i \in S^{\text{BS}} \bigcup S^{\text{NBS}};\ t \in S_{\text{T}}(k)) \tag{51}$$

$$w_{it}^{0} \le w_{i(t+1)}^{0} + w_{i(t+1)}^{1} \quad (\forall i \in S^{\text{BS}} \bigcup S^{\text{NBS}};\ t \in S_{\text{T}}(k)) \tag{52}$$

$$w_{it}^{1} \le w_{i(t+1)}^{1} + w_{i(t+1)}^{2} \quad (\forall i \in S^{\text{BS}} \bigcup S^{\text{NBS}};\ t \in S_{\text{T}}(k)) \tag{53}$$

$$w_{it}^{2} \le w_{i(t+1)}^{2} + w_{i(t+1)}^{3} \quad (\forall i \in S^{\text{BS}} \bigcup S^{\text{NBS}};\ t \in S_{\text{T}}(k)) \tag{54}$$

$$w_{it}^{3} \le w_{i(t+1)}^{3} \quad (\forall i \in S^{\text{BS}} \bigcup S^{\text{NBS}};\ t \in S_{\text{T}}(k)) \tag{55}$$

$$w_{i0}^{0} = 1 \quad (\forall i \in S^{\text{NBS}}) \tag{56}$$

$$w_{it}^{0} = 0 \quad (\forall i \in S^{\text{BS}};\ t \in S_{\text{T}}(k)) \tag{57}$$

$$w_{iT}^{3} = 1 \quad (\forall i \in S^{\text{BS}} \bigcup S^{\text{NBS}}) \tag{58}$$

$$\begin{cases} 0 \le v_{it}^{1} - (w_{it}^{1} - w_{i(t+1)}^{1}) \le 2z_{it}^{1} \\ 0 \le v_{it}^{1} - (w_{i(t+1)}^{1} - w_{it}^{1}) \le 2u_{it}^{1} \quad (\forall i \in S^{\text{NBS}};\ t \in S_{\text{T}}(k)) \\ u_{it}^{1} + z_{it}^{1} = 1 \end{cases} \tag{59}$$

$$\begin{cases} 0 \le v_{it}^{2} - (w_{it}^{1} - w_{i(t+1)}^{1}) \le 2z_{it}^{2} \\ 0 \le v_{it}^{2} - (w_{i(t+1)}^{1} - w_{it}^{1}) \le 2u_{it}^{2} \quad (\forall i \in S^{\text{BS}};\ t \in S_{\text{T}}(k)) \\ u_{it}^{2} + z_{it}^{2} = 1 \end{cases} \tag{60}$$

$$\begin{cases} 0 \le v_{it}^{3} - (w_{it}^{2} - w_{i(t+1)}^{2}) \le 2z_{it}^{3} \\ 0 \le v_{it}^{3} - (w_{i(t+1)}^{2} - w_{it}^{2}) \le 2u_{it}^{3} \quad (\forall i \in S^{\text{BS}} \bigcup S^{\text{NBS}}; t \in S_{\text{T}}(k)) \\ u_{it}^{3} + z_{it}^{3} = 1 \end{cases} \tag{61}$$

$$\sum_{t=0}^{T-1} v_{it}^{1} = 2 \quad (\forall i \in S^{\text{NBS}}) \tag{62}$$

$$\sum_{t=0}^{T-1} v_{it}^{2} = 1 \quad (\forall i \in S^{\text{BS}}) \tag{63}$$

$$\sum_{t=0}^{T-1} v_{it}^{3} = 2 \quad (\forall i \in S^{\text{BS}} \bigcup S^{\text{NBS}}) \tag{64}$$

$$\sum_{t=0}^{T} w_{it}^{0} = t_i^{\text{start}} - 1 \quad (\forall i \in S^{\text{BS}} \bigcup S^{\text{NBS}}) \tag{65}$$

$$\sum_{t=0}^{T} w_{it}^{1} = t_i^{\mathrm{crk}} \quad (\forall i \in S^{\mathrm{BS}} \bigcup S^{\mathrm{NBS}}) \tag{66}$$

$$\sum_{t=0}^{T} w_{it}^{2} = T_i^{\mathrm{R}} \quad (\forall i \in S^{\mathrm{BS}} \bigcup S^{\mathrm{NBS}}) \tag{67}$$

$$\begin{aligned} P_{it}^{\mathrm{G}} = & -(w_{it}^{1} + w_{it}^{2} + w_{it}^{3}) P_i^{\mathrm{crk}} + w_{it}^{2} R_i (t - t_i^{\mathrm{crk}}) - R_i \sum_{t=0}^{T} y_{it} \\ & + w_{it}^{3} P_i^{\max} \quad (\forall i \in S^{\mathrm{BS}} \bigcup S^{\mathrm{NBS}};\ t \in S_{\mathrm{T}}(k)), \end{aligned} \tag{68}$$

$$\begin{cases} y_{it} \geq w_{it}^{2} + w_{it}^{0} - 1 \\ y_{it} \leq w_{it}^{0} \\ y_{it} \leq w_{it}^{2} \end{cases} \quad (\forall i \in S^{\mathrm{BS}} \bigcup S^{\mathrm{NBS}};\ t \in S_{\mathrm{T}}(k)) \tag{69}$$

$$P_t^{\mathrm{main}} = \sum_{i \in S^{\mathrm{NBS}} \bigcup S^{\mathrm{BS}}} P_{it}^{\mathrm{G}} \geq 0 \quad (t \in S_{\mathrm{T}}(k)) \tag{70}$$

$$t_i^{\min} \leq t_i^{\mathrm{start}} \quad (\forall i \in S^{\mathrm{NBS}}) \tag{71}$$

$$t_i^{\mathrm{start}} \leq t_i^{\max} \quad (\forall i \in S^{\mathrm{NBS}}) \tag{72}$$

$$\tau_{\sigma(p,i)^{m^*}} \leq t_i^{\mathrm{start}} \quad (\forall i \in S^{\mathrm{NBS}}). \tag{73}$$

The objective of the MPC-MILP is represented by (49), where $S_0^{\mathrm{start}} = \varnothing$; $S_{\mathrm{T}}(k)=\{(k\text{-}1)N_{\mathrm{T}}, (k\text{-}1)N_{\mathrm{T}}+1, (k\text{-}1)N_{\mathrm{T}}+2, \ldots, T\}$; $i \in S^{\mathrm{NBS}} \setminus \bigcup_{l=0}^{k-1} S_l^{\mathrm{start}}$ represents that in each interval N_{T} the units restored in the previous time interval are removed from the NBSU set, and the unrestored units are reserved and their start-up sequence will be optimized in the current interval.

The constraints include (50) to (73) for the concerned power system, (42) to (48), wherein $t \in S_{\mathrm{T}}(k)$, for the curtailed loads of MBSRs, and the MSs related ones of MBSRs [37].

The GSUS is optimized recursively in each interval N_{T} until all the NBSUs are restored. The overall procedures of the proposed MPC based GSUS optimization strategy can be illustrated by Fig. 5.

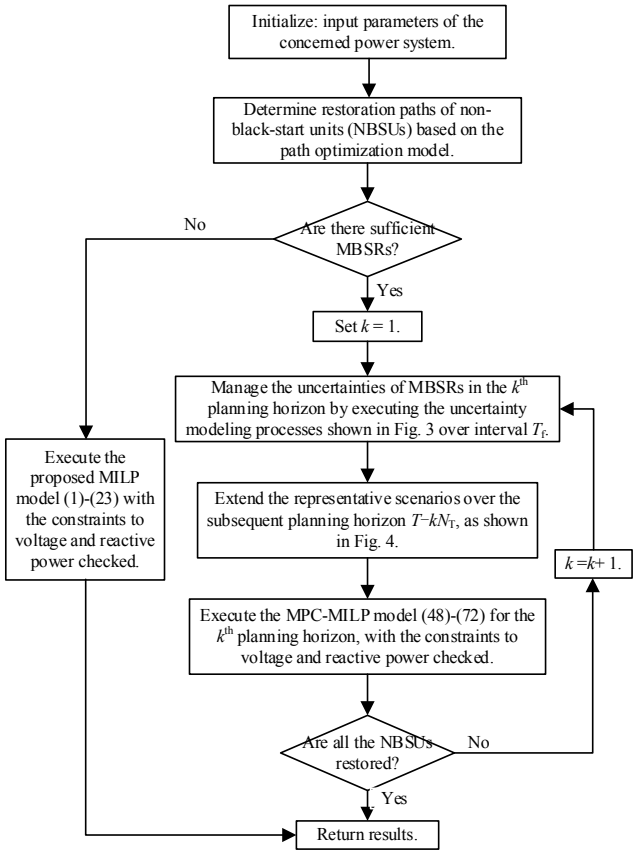

Fig. 5. Flow chart of the overall procedures of the proposed MPC based GSUS optimization strategy

V. Case Study

The proposed MPC-MILP for GSUS is solved in this work by commercial solver Gurobi 8.0.0 programmed via Python language. The modified IEEE 118 bus system with MGs and Zhejiang provincial power system in China are served for demonstration. The simulations are performed on a personal computer with Intel-i7 3.4GHz Xeon CPU and 8 GB RAM.

A. IEEE 118-Bus System with MGs

The modified IEEE 118-bus system with MGs is utilized to illustrate the proposed MPC-MILP for GSUS optimization strategy with MBSRs. The sectionalization result of the system in [38] (as shown in Fig. 6) is adopted for demonstrating parallel restoration strategy based on the proposed methods. Parameters of this system are shown in Table I, in which CBSUs locate in buses 12, 25, 59, 66 and 100. In the modified system, MGs locate in buses 5, 59, 67 and 100, and the installed capacities (ICs) of the MSs and the power of loads are shown in Table II. The ramping rate of each MG is assumed large enough that it can attain maximum output within a time step. The charging efficiency, discharging efficiency and the minimum energy capacity of ESSs are 0.85, 0.85 and 0.2, respectively. The available capacity of ESSs after the blackout is assumed as their installed energy capacity. The RESs and DLs are forecast based on historical data, whereas the UL in each MG is constant. Discretized PDFEs of RESs and loads in T_{f} are shown in Table III. The times of restoration of BSUs, energization of transmission lines, synchronization of subsystems, and parallel of reactive power compensation facilities (RPCFs) are assumed as 10, 5, 20 and 5 minutes, respectively. The NBSUs are cranked immediately upon energizing the buses they are connected to. An entire simulated blackout occurred at 14:00 (t=0) in the power system, and all the MGs was transferring into islanded operation mode and prepared to assist the PSR. The time step is set as 5 min, T_{f}=60 min, and N_{T}=45 min.

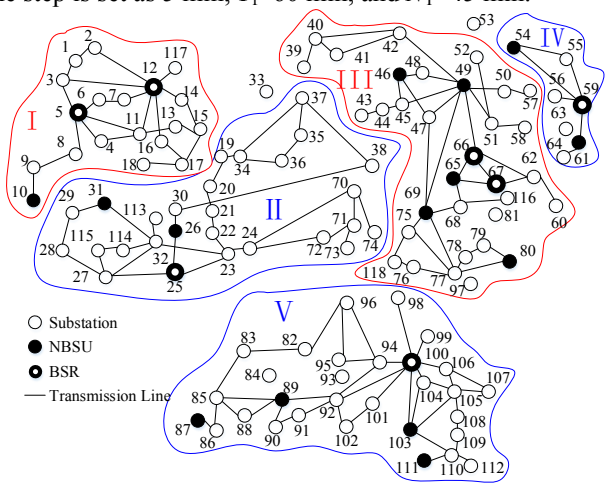

Fig. 6. The IEEE 118-bus system with sectionalization result

The optimized restoration actions using MBSRs are shown in Table IV. In Table IV, S1, …, S5 represent the set of restoration actions at each time step for subsystems I, …, V. The subscript in the action set represents the time delay of energizing some transmission line caused by overvoltage. For

example, 49-45$_{20}$ at t=40 in S3 represents a delay of 20 minutes caused by overvoltage. In the subsystem I, MG is a backup BSR. However, due to the shortage of cranking power, MG 5 energizes part of transmission lines and parallels the RPCF between BSU 12 and NBSU 10, which remarkably accelerates the restoration process after BSU 12 is restored. In the subsystem II, there is no MBSR and BSU 25 restores this section. In the subsystem III, the BSU and MG cooperate with each other to restore the subsystem. At the beginning of restoration when BSU 66 is unavailable, MG 67 is the only BSR and it energizes some transmission lines and provides NBSU 49 with cranking power. After BSU 66 is restored, MG 67 and BSU 66 cooperatively crank the rest units. In the subsystem IV, with constraints met, the MBSR provides NBSUs 54 and 61 with cranking power immediately after the blackout. In the subsystem V, due to the critical minimum time requirement, NBSU 103 cannot be restored immediately, but part of lines are energized and NBSU 111 is restored first by the MBSR. The NBSUs' start time (ST) is shown in Table I.

TABLE I
UNIT PARAMETERS OF THE IEEE 118-BUS SYSTEM

Gen. No.	P^{max} (MW)	P^{crk} (MW)	R(MW /hr)	t^{max} (min)	t^{min} (min)	t^{crk} (min)	ST (min)
10	550	15	200	N/A	30	40	40
12	**185**	**0**	**90**	**N/A**	**N/A**	**20**	**-**
25	**320**	**0**	**180**	**N/A**	**N/A**	**25**	**-**
26	414	12	180	50	N/A	35	45
31	107	3	60	N/A	N/A	30	70
46	119	3	60	N/A	N/A	25	45
49	304	10	180	N/A	N/A	35	15
54	148	5	60	N/A	N/A	35	10
59	**255**	**0**	**90**	**N/A**	**N/A**	**20**	**-**
61	260	8	90	N/A	N/A	30	10
65	491	12.5	200	N/A	20	35	35
66	**492**	**0**	**250**	**N/A**	**N/A**	**15**	**-**
69	805.2	20	420	120	N/A	40	40
80	577	15	200	N/A	N/A	40	55
87	104	3	60	N/A	N/A	35	70
89	707	16	400	N/A	N/A	40	60
100	**352**	**0**	**180**	**N/A**	**N/A**	**25**	**-**
103	140	4	60	N/A	35	30	40
111	136	4	60	N/A	N/A	30	25

TABLE II
MG PARAMETERS OF THE IEEE 118-BUS SYSTEM AND ZPPS

Parm. /No.	5	59	67	100	I	II	III	IV
IC of WT (MW)	4	5	4	10	20	10	0	30
IC of PV (MW)	2	8	2	5	50	30	25	30
IC of DU (MW)	10	12	10	10	20	15	20	10
P^{dcmax} /P^{chmax}	4	5	4	5	8	10	10	8
E^{max} (MWh)	10	10	10	15	32	20	20	20
Max. DL (MW)	10	10	10	12	36	22	28	28
UL (MW)	3	7.5	0	12	15	14	5	16

TABLE III
DISCRETIZED PDFES FOR THE IEEE 118-BUS SYSTEM AND ZPPS

Prob.	FE of WT (%)	Prob.	FE of PV (%)	Prob.	FE of DL (%)
0.15	-10	0.2	-5	0.3	3
0.3	-5	0.25	-2.5	0.4	0
0.1	0	0.1	0	0.3	3
0.3	5	0.25	2.5	-	-
0.15	10	0.2	5	-	-

TABLE IV
RESTORATION ACTIONS FOR THE IEEE 118-BUS SYSTEM

Time (min)	Restoration Actions
5	S1={MG 5 is islanded, Crank BSU 12}; S2={Crank BSU 25}; S3={Crank BSU 66, MG 67 is islanded}; S4={MG 59 is islanded}; S5={MG 100 is islanded}
10	S1={Energize line 5-11,5-8}; S3={Energize line 67-66}; S4={Energize line 59-54, 59-61, Crank NBSU 54, 61}; S5={Energize line 100-103, 100-92}
15	S1={Parallel RPCF 8}; S3={Energize line 66-49, Crank NBSU 49}; S5={Energize line 103-110, Parallel RPCF 92}
20	S1={Energize line 8-9, 11-12}; S3={BSU 66 is cranked}; S5={Parallel RPCF 110}
25	S1={BSU 12 is cranked}; S5={Energize line 110-111, Crank NBSU 111}
30	S2={BSU 25 is cranked}; S3={BSU 66 is restored and paralleled with MG 67 at bus 66}
35	S1={BSU 12 is restored and paralleled with MG 5 in bus 12}; S3={Energize line 66-65, Crank NBSU 65}
40	S1={Energize line 9-10, Crank NBSU 10}; S2={BSU 25 is restored}; S3={Energize line 49-45$_{20}$, 49-69, Crank NBSU 69}; S4={NBSU 61 is restored}; S5={Crank NBSU 103}
45	S1={Energize line 12-16}, S2={Energize line 25-26, Crank NBSU 26}; S3={Energize line 45-46, 69-77, Crank NBSU 46}; S4={NBSU 54 is restored}
50	S1={Energize line 16-17}; S2={Energize line 25-27$_5$}; S3={Parallel RPCF 77, NBSU 49 is restored}; S5={Energize line 92-89}
55	S2={Parallel RPCF 27}; S3={Energize line 77-80, Crank NBSU 80}; S4={Energize line 54-49}; S5={Energize line 89-85, NBSU 111 is restored}
60	S2={Energize line 27-32}; S5={Parallel RPCF 85, Crank NBSU 89}
65	S2={Parallel RPCF 32}; S5={Energize line 85-86}
70	S2={Energize line 32-31, Crank NBSU 31}; S3={NBSU 65 is restored}; S5={Energize line 86-87, Crank NBSU 87}
75	S5={Energize line 100-99}
80	S2={NBSU 26 is restored}
85	S2={Energize line 26-30}
90	S2={Energize line 30-38, 30-17}
95	S3={Energize line 65-38, NBSU 80 is restored}
100	S3={Energize line 80-99}

Although the MGs can restore the systems, part of loads of MBSRs might be curtailed. The load curtailment of MG 5 is near zero. The energy losses of MGs 59 and 67 are about 0.185 and 0.151 MWh respectively as a result of DLs' curtailment. Although the load losses in MGs 5, 59 and 67 are negligible, MG 100 in subsystem V curtails substantial amount of loads. The energy losses of MG 100 during restoration are about 3.173 MWh (2.866 MWh for DLs and 0.307 MWh for ULs). The curtailment of loads is a synthesized effect of generation of MSs, demand of loads, and the restoration actions. If the output of a MBSR is insufficient to satisfy the demands of local loads and the cranking power of NBSUs, part of loads of the MBSR might be curtailed to restore the system.

The generator STs optimized in the first interval (k=1) for NBSUs 87, 89, 103 and 111 are at 70, 65, 40 and 25 min, respectively. However, in the second interval (k=2) along with the planning horizon, the GSUS model is re-optimized based on the previous NBSU states, the newly forecast parameters and generated scenarios. The attained STs of NBSUs 89 and 87 are at 60 and 70 min, respectively. Thus in the restoration actions, NBSUs 111, 103, 89 and 87 are cranked at 25, 40, 60 and 70 min, respectively. The load curtailment of the first and second intervals is 2.148/0.005 MWh for DLs/ULs and 2.866/0.305

MWh for DLs/ULs, respectively. However, the objective values of the GSUS model optimized at k=1 and k=2 are 127.93 and 127.74 respectively, which means that the optimization result is improved by the MPC technique. While the MPC technique improves optimization result in subsystem V effectively, the advantages are not fully reflected in other subsystems due to the sufficient cranking power from BSUs and/or MBSRs in the subsequent intervals following the first one. As a result, the MPC technique can mitigate the inaccuracy of forecast power of MBSRs caused by long FTH and improve the optimization results.

It can be concluded that the MGs can effectively restore the system by the proposed MPC-MILP. To further demonstrate the proposed method, generation capabilities (GCs) and the restored energy of the proposed MPC-MILP, MBMILP [6], generator startup sequencing model (GSSM) [10], and FA [11], attained by utilizing MBSRs, are compared in Fig. 7 and Table V, respectively. It can be seen from Fig. 7 that in subsystems I and V the GC of MPC-MILP is larger than that attained by the MBMILP, FA and GSSM. In subsystem II where no MBSR is considered, the MPC-MILP degenerates to the MILP model as in Section II and it attains a GC as good as the other three methods. In subsystem III, the MPC-MILP method attains the same GC as MBMILP and GSSM methods, whereas the least GC is attained by the FA. In subsystem IV, all of the four methods attain the same GC. In subsystem V, the MPC-MILP method outperforms the other three methods, while the MBMILP and GSSM achieve moderate GCs and the FA method performs the worst and attains the least GC.

methods are optimal for their corresponding models respectively and are better than the result of the FA method which utilizes heuristic optimization algorithm thus the optimum cannot be guaranteed. On the other hand, the MPC-MILP, MBMILP and GSSM methods utilize different restoration path optimization models to find the restoration paths for NBSUs, i.e., the MBMILP method utilizes power transfer distribution factor (PTDF) to search restoration paths, whereas the GSSM method utilizes the Dijkstra algorithm of complex network theory. Since the PTDF may not find the shortest restoration path and the Dijkstra algorithm does not consider the overvoltage risks of energizing lines although it can find the shortest path, these path optimization models may be suboptimal on some conditions and may undermine the overall GC optimized. For example, the restoration paths for the subsystem I optimized by the MPC-MILP, MBMILP and GSSM methods are [12→11→5→8→9→10], [12→11→4→5→8→9→10], and [12→3→5→8→9→10], respectively, which may result in the differences of GC in subsystem I. In subsystem V, the restoration paths for NBSU 89 and 87 are optimized as [100→92→89→85→86→87], [100→92→89→88→85→86→87] and [100→92→89→85→86→87] by the MPC-MILP, MBMILP and GSSM methods, respectively. As a result, the optimized GCs in subsystem V of the MBMILP and GSSM methods are smaller than that of the MPC-MILP method. In other words, the differences in optimization methods and restoration paths may influence the total GC of the power system concerned.

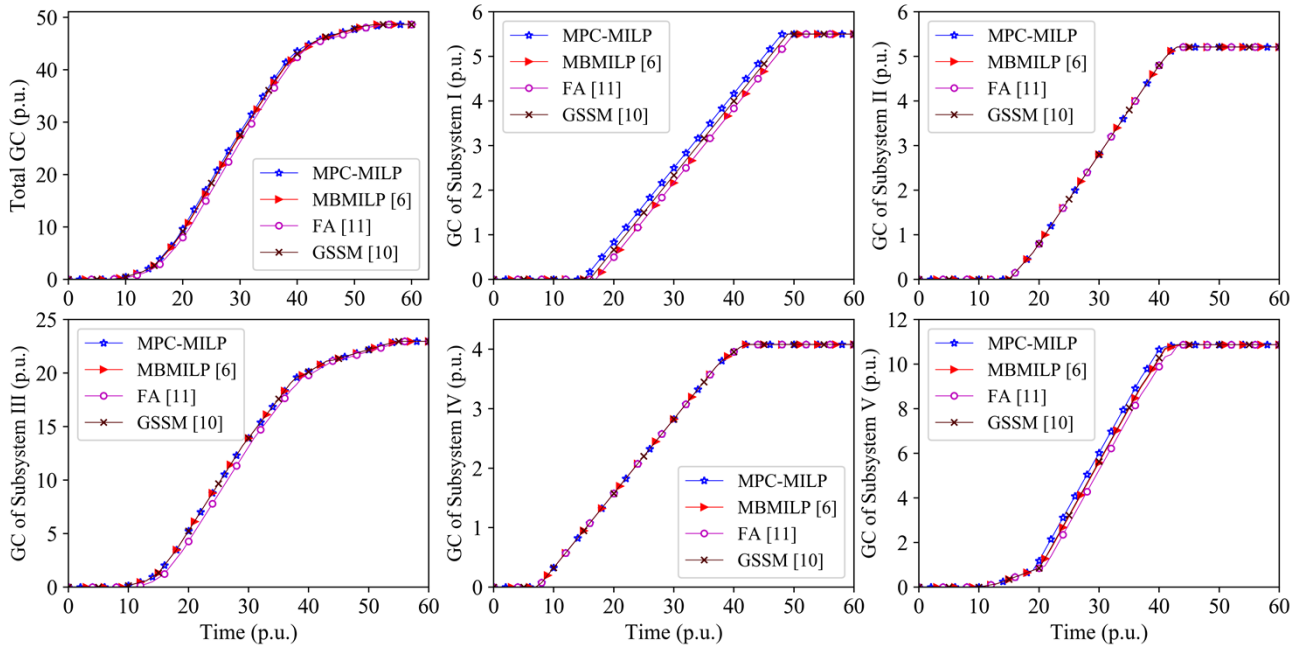

Fig. 7. Comparisons of GCs of different methods for the IEEE 118 bus system

It should be noted that the difference of GC is a synthetized effects of the optimization method utilized and the variables, parameters and constraints in the model. Since the MPC-MILP, MBMILP and GSSM methods are based on linear programming models, the optimization results of these three

As shown in Table V, the restored energy of the MPC-MILP in subsystems is larger than that of other methods. The total restored energy attained by the MPC-MILP is 13,021 MWh, and is 269, 437 and 179 MWh larger in quantity than that attained by the MBMILP, FA and GSSM, respectively, which

means more unserved loads are resupplied. As a result, the MPC-MILP outperforms the MBMILP, FA and GSSM. The optimal GSUS can be attained and more unserved loads can be resupplied by utilizing MPC-MILP.

TABLE V
THE RESTORED ENERGY OF THE IEEE 118-BUS SYSTEM (UNIT: MWH)

Subsystem	I	II	III	IV	V	Total
MPC-MILP	1329	1368	6188	1248	2888	13021
MBMILP [6]	1238	1368	6087	1248	2811	12752
FA [11]	1238	1368	5981	1248	2750	12584
GSSM [10]	1283	1368	6122	1248	2820	12842

B. *Zhejiang Provincial Power System in China*

In order to further validate the effectiveness of the proposed restoration strategy in actual power system, simulations on Zhejiang provincial power system (ZPPS) in China are performed. The capacity of ZPPS is 43, 000 MW, and about 45 percent of the capacity is required to be restored at early stages of PSR. ZPPS consists of 38 NBSUs, 369 buses and 525 transmission lines, and it is partitioned into four subsystems for parallel restoration, as shown in [39]. Four MGs (i.e., MG I, II, III, and IV) originated from the actual photovoltaic power stations in Zhejiang province are utilized as MBSRs. Details of the MBSRs are shown in Table II. Suppose that a blackout occurs at 10:00 a.m., and then all the MGs transfer into islanded operation mode and begin to restore the system. The GCs of different methods are shown in Fig. 8. The restored energy during restoration is shown in Table VI. Comparisons with the MBMILP, FA and GSSM show that the MPC-MILP attains the largest GC and the optimal GSUS. The total restored energy of the MPC-MILP over the restoration period is 49,264 MWh, and is 942, 1721 and 573 MWh larger than that of the MBMILP, FA and GSSM, respectively. In other words, application of the proposed GSUS optimization strategy to ZPPS shows that the NBSUs can be successfully restored by MBSRs, and that the optimal GSUS can be effectively determined and more unserved loads resupplied by using that strategy.

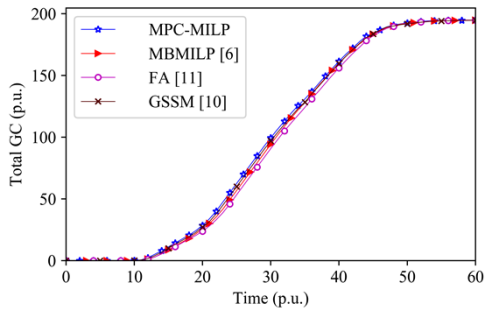

Fig. 8. Comparisons of the total GCs of different methods for ZPPS

TABLE VI
THE RESTORED ENERGY OF ZPPS (UNIT: MWH)

Subsystem	I	II	III	IV	Total
MPC-MILP	14294	13882	7810	13279	49264
MBMILP [6]	14107	13450	7633	13132	48322
FA [11]	13996	13260	7591	12697	47543
GSSM [10]	14224	13683	7643	13141	48691

VI. DISCUSSIONS AND COMPARISONS

A. *Comparison of LPSR with Fast Forward Selection*

The PMTP based LPSR outperforms the SCENRED2 tool which is based on forward selection or backward selection heuristic by iteratively adding scenarios to an initial set or removing scenarios from the initial set [27] and [30]. In order to further validate the effectiveness and efficiency of the proposed LPSR method, comparisons of the proposed LPSR with fast forward selection [28] are performed with multiple uncertainty scenario numbers. The uncertainty scenarios are generated based on the parameters of MG I in ZPPS. The cardinality of subset of representative scenarios is set as 30. Simulation results on the LPSR and fast forward selection are illustrated in Table VII.

TABLE VII
COMPARISONS OF THE PROPOSED LPSR WITH FAST FORWARD SELECTION

	LPSR		Fast Forward Selection	
Scenario number	TD	CT (s)	TD	CT (s)
1200	3.2680	7.53	3.3341	77.96
2400	3.2577	24.53	3.2908	281.67
4000	2.5585	62.78	2.5823	879.10
6500	3.2669	70.11	3.2676	2297.24
10000	3.3763	120.63	3.3826	5632.28

TD: transportation distance; CT: computing time.

It can be seen from Table VII that the transportation distance of the proposed LPSR is always smaller than that of the fast forward selection method. In other words, the LPSR method can provide a more representative uncertainty subset since the transportation distance is smaller. As the number of uncertainty scenarios increases, the computing time of the LPSR method is substantially smaller than that of the fast forward selection. That is mainly because the distance between each the pair of uncertainty scenarios is calculated for the fast forward selection, i.e., for a superset of Q original uncertainty scenarios, the fast forward selection calculates $Q \times Q$ times the distance between scenarios; whereas the LPSR calculates only $Q \times K$ times the distance between scenarios, where K represents the desired number of representative scenarios. As a result, the proposed PMTP based LPSR could effectively and efficiently deal with a large number of original uncertainty scenarios.

B. *Comparison of SHC with MPC*

In order to demonstrate the advantages and efficiency of SHC, computing times with various planning horizon for MPC and its variant SHC are compared, as shown in Table VIII, wherein T=60 p.u.. Since the optimization models for the subsystems I and II of the IEEE 118 bus system degenerate into a MILP one, the comparisons of SHC with MPC are not made for these two subsystems.

TABLE VIII
COMPARISONS OF SHC AND MPC WITH DIFFERENT PLANNING HORIZONS (UNIT: S)

	T		1.25T		1.5T	
subsystem	SHC	MPC	SHC	MPC	SHC	MPC
IEEE 118-III	9.01	9.19	13.62	16.82	18.86	26.68
IEEE 118-IV	4.56	4.55	7.00	7.01	9.24	9.31
IEEE 118-V	17.94	20.82	17.51	18.92	25.71	30.9
ZPPS-I	31.68	38.92	51.35	87.02	92.62	152.85
ZPPS -II	29.05	36.05	59.61	86.95	98.74	160.21
ZPPS -III	21.96	31.06	45.98	67.06	70.69	113.47

ZPPS -IV	15.95	20.36	54.33	66.63	80.44	123.06

As seen from Table VIII, the computing times of SHC are less than those of MPC in the three planning horizons for subsystem III and V of the IEEE 118 bus system and all the four subsystems of ZPPS. In subsystem IV of the IEEE 118 bus system, the computing times of SHC in the three planning horizons are almost equal to those of MPC, since all the NBSUs of this subsystem are cranked within the first time interval, i.e., k=1. Since the planning horizons for the SHC and MPC based methods when k=1 are the same, the computing times for these two methods should be equal to each other in theory. Therefore, it seems that the minor errors of computing times between the SHC and MPC based methods are not so much from the difference between the methods as from the model optimizations and executions. A larger planning horizon will inevitably result in more variables and parameters of the GSUS optimization model, so the computing times for both the SHC and MPC will rise as the planning horizons increase, as illustrated by Table VIII. Table VIII also demonstrates an increasing computing time reduction of the SHC technique. Although merely 2% of time is saved with the planning horizon of T in subsystem III of the IEEE 118 bus system, about 65.03% of time reduction is attainted with the planning horizon of 1.5T in subsystem V of the IEEE 118 bus system. In other words, utilizing the variant SHC technique in the GSUS optimization model is more efficient than utilizing the original MPC one.

VII. Conclusion

A generator start-up optimization strategy for PSR with MGs is proposed in this work. The GSUS problem is formulated as a MILP from a new different perspective. The variable output power of MSs and demands of MGs are modeled as scenarios based on discretization of PDFEs and formulation of PMTP. The MPC technique is utilized to mitigate the impacts of the increasing FEs of uncertainty parameters. Numerical simulations on the modified IEEE 118-bus system with MGs and the ZPPS in China demonstrate that after a big blackout the power system can be successfully restored and the GSUS can be effectively determined by the proposed MPC-MILP. However, the transient processes are not included in this work. In future works, attention will be paid to the transient processes of MGs, which will further validate the effectiveness.

References

[1] V. C. Güngör, D. Sahin, T. Kocak, S. Ergüt, C. Buccella, C. Cecati, G. P. Hancke, "Smart grid technologies: communication technologies and standards," *IEEE Trans. Ind. Informat*., vol. 7, no. 4, pp. 529–539, Nov. 2011.

[2] M. Ayar, S. Obuz, R. D. Trevizan, A. S. Bretas, H. A. Latchman, "A distributed control approach for enhancing smart grid transient stability and resilience," *IEEE Trans. Smart Grid*, vol. 8, no. 6, pp. 3035–3044, Nov. 2017.

[3] M. Ayar, R. D. Trevizan, S. Obuz, A. S. Bretas, H. A. Latchman, N. G. Bretas, "Cyber-physical robust control framework for enhancing transient stability of smart grids," *IET Cyber-Phys. Syst., Theory Appl.*, vol. 2, no. 4, pp. 198–206, Dec. 2017.

[4] J. Feltes and C. Grande-Moran, "Down, but not out: A brief overview of restoration issues," *IEEE Power Energy Mag.*, vol. 12, no. 1, pp. 34–43, Jan./Feb. 2014.

[5] A. S. Bretas, A. G. Phadke, "Artificial neural networks in power system restoration," *IEEE Trans. Power Del.*, vol. 18, no. 4, pp. 1181–1186, Oct. 2003.

[6] W. Sun, C.-C. Liu, and L. Zhang, "Optimal start-up strategy for bulk power system restoration," *IEEE Trans. Power Syst.*, vol. 26, no. 3, pp. 1357–1366, Aug. 2011.

[7] Y. Hou, C.-C. Liu, K. Sun, P. Zhang, S. Liu, D. Mizumura, "Computation of milestones for decision support during system restoration," *IEEE Trans. Power Syst.*, vol. 26, no. 3, pp. 1399–1409, Jun. 2011.

[8] Y.-T Chou, C.-W. Liu, Y.-J. Wang, C.-C Wu, C.-C. Lin, "Development of a black start decision supporting system for isolated power systems." *IEEE Trans. Power Syst.*, vol. 28, no. 3, pp.2202–2210, Aug. 2013.

[9] A. Golshani, W. Sun, Q. Zhou, Q. P. Zheng, J. Tong, "Two-stage adaptive restoration decision support system for a self-healing power grid," *IEEE Trans. Ind. Informat*., vol. 13, no. 6, pp. 2802-2812, Dec. 2017.

[10] F. Qiu, and P. Li, "An integrated approach for power system restoration planning," *Proc. IEEE*, vol. 105, no. 7, pp. 1234–1252, Jul. 2017.

[11] A. M. El-Zonkoly, "Renewable energy sources for complete optimal power system black-start restoration," *IET Gener. Transm. Distrib.*, vol. 9, no. 6, pp. 531–539, 2015.

[12] H. Gao, Y. Chen, Y. Xu, and C.-C. Liu, "Resilience-oriented critical load restoration using microgrids in distribution systems," *IEEE Trans. Smart Grid*, vol. 7, no. 6, pp. 2837–2848, Nov. 2016.

[13] Y. Xu, C.-C. Liu, K. P. Schneider, F. K. Tuffner, D. T. Ton, "Microgrids for service restoration to critical load in a resilient distribution system," *IEEE Trans. Smart Grid*, vol. 9, no. 1, pp. 426–437, Jan. 2018.

[14] Z. Wang, J. Wang, "Service restoration based on AMI and networked microgrids under extreme weather events," *IET Gener. Transm. Distrib.*, vol. 11, no. 2, pp. 401–408, 2017.

[15] A. Castillo, "Microgrid provision of blackstart in disaster recovery for power system restoration," in *Proc. 2013 IEEE Int. Conf. Smart Grid Commun.*, Vancouver, BC, Canada, 2013, pp. 534–539.

[16] K. P. Schneider, F. K. Tuffner, M. A. Elizondo, C.-C. Liu, Y. Xu, and D. Ton, "Evaluating the feasibility to use microgrids as a resiliency resource," *IEEE Trans. Smart Grid*, vol. 8, no. 2, pp. 687–696, Mar. 2017.

[17] R. Diestel, *Graph Theory*, 4th ed. Berlin, Germany: Springer, 2017.

[18] Z. Ren, F. Shao, J. Liu, Q. Guo, B. Wang, "Node importance measurement based on the degree and clustering coefficient information," *Acta Phys. Sin.*, vol. 62, no. 12, pp. 128901, 2013.

[19] S. Moayedi and A. Davoudi, "Distributed tertiary control of DC microgrid clusters," *IEEE Trans. Power Electron.*, vol. 31, no. 2, pp. 1717–1733, Feb. 2016.

[20] A. J. von Appen, C. Marnay, M. Stadler, I. Momber, D. Klapp, A. von Scheven., "Assessment of the economic potential of microgrids for reactive power supply," in *Proc. IEEE 8th Int. Conf. Power Electron. ECCE Asia (ICPE & ECCE)*, Jeju, Korea, 2011, pp. 809–816.

[21] C. L. Moreira, F. O. Resende, and J. A. P. Lopes, "Using low voltage MicroGrids for service restoration," *IEEE Trans. Power Syst.*, vol. 22, no. 1, pp. 395–403, Feb. 2010.

[22] W. Liu, W. Gu, Y. Xu, Y. Wang, K. Zhang, "General distributed secondary control for multi-microgrids with both PQ-controlled and droop-controlled distributed generators," *IET Gener. Transm. Distrib.*, vol. 11, no. 3, pp. 707–718, 2017.

[23] A. Fabbri, T. G. S. Roman, J. R. Abbad, and V.M. Quezada, "Assessment of the cost associated with wind generation prediction errors in a liberalized electricity market," *IEEE Trans. Power Syst.*, vol. 20, no. 3, pp. 1440–1446, Aug. 2005.

[24] M. Peik-Herfeh, H. Seifi, and M. Sheikh-El-Eslami, "Decision making of a virtual power plant under uncertainties for bidding in a day-ahead market using point estimate method," *Int. J. Elect. Power Energy Syst.*, vol. 44, no. 1, pp. 88–98, 2013.

[25] Q. Zhao, Y. Shen, and M. Li, "Control and bidding strategy for virtual power plants with renewable generation and inelastic demand in electricity markets," *IEEE Trans. Sustain. Energy*, vol. 7, no. 2, pp. 562–575, Apr. 2016.

[26] A. Y. Saber and G. K. Venayagamoorthy, "Resource scheduling under uncertainty in a smart grid with renewables and plug-in vehicles," *IEEE Syst. J.*, vol. 6, no. 1, pp. 103–109, Mar. 2012.

[27] H. Heitsch, and W. Römisch, "Scenario reduction algorithms in stochastic programming," *Comput. Optim. Appl.*, vol. 24, no. 2–3, pp. 187–206, Feb. 2003.

[28] N. Growe-Kuska, H. Heitsch, and W. Romisch, "Scenario reduction and scenario tree construction for power management problems," in *Proc. IEEE Bologna Power Tech Conf.*, Bologna, Italy, 2003, pp. 1–7.

[29] Y. Wang, Y. Liu, and D. S. Kirschen, "Scenario reduction with submodular optimization," *IEEE Trans. Power Syst.*, vol. 32, no. 3, pp. 2479–2480, May 2017.

[30] Z. Z. Li, and Z. K. Li, "Linear programming-based scenario reduction using transportation distance," *Comput. Chem. Eng.*, vol. 88, pp. 50–58, May 2016.
[31] R. M. Kovacevic and A. Pichler, "Tree approximation for discrete time stochastic processes: a process distance approach," *Ann. Oper. Res.*, vol. 235, no. 1, pp. 395–421, Sep. 2015.
[32] F. Allgower, R. Findeisen, and Z. K. Nagy, "Nonlinear model predictive control: From theory to application," *J. Chin. Inst. Chem. Eng.*, vol. 35, no. 3, pp. 299–315, 2004.
[33] A. Parisio and L. Glielmo, "Stochastic model predictive control for economic/environmental operation management of microgrids," in *Proc. Eur. Control Conf.*, Zürich, Switzerland, Jul. 2013, pp. 2014–2019.
[34] D. E. Olivares, J. D. Lara, C. A. Cañizares, and M. Kazerani, "Stochastic predictive energy management system for isolated microgrids," *IEEE Trans. Smart Grid*, vol. 6, no. 6, pp. 2681–2693, Nov. 2015.
[35] K. Meng, Z. Y. Dong, Z. Xu, S. R. Weller, "Cooperation-driven distributed model predictive control for energy storage systems," *IEEE Trans. Smart Grid*, vol. 6, no. 6, pp. 2583–2585, Nov. 2015.
[36] M. M. Thomas, J. L. Kardos, and B. Joseph, "Shrinking horizon model predictive control applied to autoclave curing of composite laminate materials," in *Proc. Amer. Control Conf.*, vol. 1. Baltimore, MD, USA, Jun. 1994, pp. 505–509.
[37] S. Talari, M. Yazdaninejad, and M.-R. Haghifam, "Stochastic-based scheduling of the microgrid operation including wind turbines, photovoltaic cells, energy storages and responsive loads," *IET Gener. Transm. Distrib.*, vol. 9, no. 12, pp. 1498–1509, 2015.
[38] W. Liu, Z. Lin, F. Wen, C. Y. Chung, Y. Xue, G. Ledwich, "Sectionalizing strategies for minimizing outage durations of critical loads in parallel power system restoration with bi-level programming," *Int. J. Elec. Power*, vol. 71, pp. 327–334, Oct. 2015.
[39] L. Sun, C. Zhang, Z. Lin, F. Wen, Y. Xue, M. A. Salam, S. P. Ang, "Network partitioning strategy for parallel power system restoration," *IET Gener. Transm. Distrib.*, vol. 10, no. 8, pp. 1883–1892, 2016.

Yuxuan Zhao received the B.E. degree in electrical engineering from Northeast Electric Power University, Jilin, China, in 2013. He is currently pursuing his PhD degree in electrical engineering in the College of Electrical Engineering at Zhejiang University, Hangzhou, China. His current research interests are renewable energy operation and planning, and power system restoration.

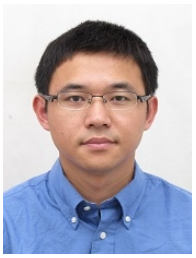

Zhenzhi Lin received the Ph.D. degree in electrical engineering from South China University of Technology, Guangzhou, China, in 2008.

He was a Research Assistant in the Department of Electrical Engineering at The Hong Kong Polytechnic University from 2007 to 2008, a Research Scholar in the Min Kao Department of Electrical Engineering and Computer Science at the University of Tennessee from 2010 to 2011, and a Research Associate in School of Engineering and Computing Sciences at Durham University from 2013 to 2014. He is currently an Associate Professor in the School of Electrical Engineering, Zhejiang University, Hangzhou, China. His research interests include power system wide-area monitoring and control, controlled islanding and power system restoration.

Yi Ding (M'12) received the B.Eng. degree from Shanghai Jiaotong University, Shanghai, China, in 2000, and the Ph.D. degree from Nanyang Technological University (NTU), Singapore, in 2007, both in electrical engineering.

He is a Professor in the College of Electrical Engineering, Zhejiang University (ZJU), China. Before joining ZJU, he was an Associate Professor in the Department of Electrical Engineering, Technical University of Denmark (DTU), Denmark. He also held research and teaching positions in University of Alberta, Canada and NTU. He was a Consultant as Energy Economist for Asian Development Bank in 2010. He is editorial member of international journals of Electric Power System Research and Journal of Modern Power Systems and Clean Energy. He is also a Guest Editor for the special section of IEEE Trans. on Power Systems. He is a member of IEC working groups for micro-grid standards. His research areas include power system planning and reliability evaluation, smart grid and complex system risk assessment.

Yilu Liu received the B.S. degree from Xian Jiaotong University, Xi'an, China, and the M.S. and Ph.D. degrees from the Ohio State University, Columbus, OH, USA, in 1986 and 1989, respectively.

She was currently the Governor's Chair with the University of Tennessee, Knoxville, TN, USA, and Oak Ridge National Laboratory (ORNL). She was elected as the member of National Academy of Engineering in 2016. She is also the Deputy Director of the DOE/NSF co-funded engineering research center CURENT. Prior to joining UTK/ORNL, she was a Professor at Virginia Tech. She led the effort to create the North American power grid frequency monitoring network at Virginia Tech, which is now operated at UTK and ORNL as Grid-Eye. Her current research interests include power system wide-area monitoring and control, large interconnection-level dynamic simulations, electromagnetic transient analysis, and power transformer modeling and diagnosis.

Lei Sun received his Ph.D. degree in electrical engineering from Zhejiang University, China, in 2017. He was a visiting Ph.D. student at Technical University of Denmark from 2015 to 2016. He is currently a lecturer in the School of Electrical Engineering and Automation, Hefei University of Technology, China.

His research interests include power system restoration, distribution automation and reliability analysis.

Yong Yan received the B.S. and the M.S. degrees from Chongqing University, Chongqing, China, and South China University of Technology, Guangzhou, China, in 2006 and 2009, respectively. He is currently pursuing his PhD degree in electrical engineering in the College of Energy and Electrical Engineering at Hohai University, China. His current research interests are blockchain, artificial intelligence, and power system.